Original Article

Cytogenetic and Genome Research

Cytogenet Genome Res 2009;125:186–200
DOI: 10.1159/000230003

Accepted after revision: May 13, 2009
by M. Schmid

Targeted Disruption of the Mouse *Npal3* Gene Leads to Deficits in Behavior, Increased IgE Levels, and Impaired Lung Function

P. Grzmil[a, b] J. Konietzko[a] D. Boehm[a] S.M. Hoelter[c] A. Aguilar[d, e] A. Javaheri[d, e] S. Kalaydjiev[d, f, g] T. Adler[d, f] I. Bolle[h] I. Adham[a] C. Dixkens[a] S. Wolf[a] H. Fuchs[d] V. Gailus-Durne[d] W. Wurst[c, i] M. Ollert[e] D. Busch[f] H. Schulz[h] M. Hrabe de Angelis[d, i] P. Burfeind[a]

[a]Institute of Human Genetics, University of Goettingen, Goettingen, Germany; [b]Department of Genetics and Evolution, Institute of Zoology, Jagiellonian University, Cracow, Poland; [c]Institute of Developmental Genetics, Helmholtz Zentrum München, and [d]German Mouse Clinic, GSF Forschungszentrum für Umwelt und Gesundheit GmbH, Neuherberg, [e]Division of Environmental Dermatology and Allergy (UDA), Helmholtz Zentrum München/ Technische Universität München, and Clinical Research Division of Molecular and Clinical Allergotoxicology, Department of Dermatology and Allergy, Technische Universität München, [f]Institute for Medical Microbiology, Immunology and Hygiene, Technische Universität München, München, Germany; [g]Faculty of Life Sciences, Michael Smith Building, The University of Manchester, Manchester, UK; [h]Institute of Lung Biology and Disease, Helmholtz Zentrum München, Neuherberg, [i]Chair of Developmental Genetics, Center of Life and Food Sciences Weihenstephan, Technische Universität München, Freising, Germany

Key Words
Atopic disease · Behavior · Immune system · *Npal3* knockout mice · Phenotypic analyses

Abstract
The non-imprinted in Prader-Willi/Angelman syndrome (NIPA) proteins are highly conserved receptors or transporters. Translocation of *NIPA* genes were found in patients with Prader-Willi syndrome, and loss-of-function of the *NIPA1* gene was identified in hereditary spastic paraplegia. The family of NIPA-like domain containing (NPAL) proteins is closely related to the NIPA proteins, but to date nothing is known about their function. Here, we could demonstrate that both human *NPAL3* and mouse *Npal3* are ubiquitously expressed and encode highly conserved proteins. To further elucidate the function of the *Npal3* gene, knockout *(Npal3*$^{-/-}$*)* mice were generated. Intensive phenotypic analyses revealed that disruption of the *Npal3* gene results in a pleiotropic phenotype. The function of the nervous system was impaired in both mutant males and females which could be demonstrated in behavioral tests. In addition, in *Npal3* mutants the number of NK cells was decreased and changes in IgM, IgG_2, and IgA were observed, indicating that the immune system is also affected. Interestingly, increased IgE levels as well as impaired lung functions were observed in mutant males but not in mutant females. It should be noted that the human *NPAL3* gene is located at 1p36.12→p35.1, and atopic diseases were previously linked to this genomic region. Thus, the *Npal3*$^{-/-}$ mice could serve as a valuable model system for studying atopic diseases.

The *NIPA* (non-imprinted in Prader-Willi/Angelman syndrome) genes encode highly conserved proteins which function as receptors or transporters. Both *NIPA1* and *NIPA2* genes are located on human chromosome 15

KARGER

Fax +41 61 306 12 34
E-Mail karger@karger.ch
www.karger.com

1424–8581/09/1253–0186$26.00/0

Accessible online at:
www.karger.com/cgr

Dr. Peter Burfeind
Institute of Human Genetics
University of Goettingen, Heinrich-Dueker-Weg 12
DE–37073 Göttingen (Germany)
Tel. +49 551 397 595, Fax +49 551 399 303, E-Mail pburfei@gwdg.de

among about 30 imprinted genes involved in the Prader-Willi/Angelman syndrome (OMIM 608145, 608146) [Butler, 1990; Nicholls et al., 1993; Nicholls and Knepper, 2001; Chai et al., 2003; Butler et al., 2004]. Furthermore, the *NIPA1* gene has also been implicated in another distinct human disorder termed autosomal dominant hereditary spastic paraplegia (ADHSP, OMIM 600363) [Rainier et al., 2003]. In this study the discovery of a dominant negative mutation in the *NIPA1* gene was reported in a kindred with ADHSP, linked to chromosome 15q11→q13 (SPG6 locus). Both *NIPA1* and *NIPA2* genes are ubiquitously expressed; however, for the *NIPA1* gene it was demonstrated that it is highly expressed in neuronal tissues. The NIPA proteins contain conserved transmembrane domains, and for both NIPA1 and NIPA2 it was shown that they function as Mg^{2+} ion transporters [Goytain and Quamme 2005; Goytain et al., 2007, 2008].

Closely related to the NIPA proteins is the putative NIPA-like domain containing (NPAL) protein family which consists so far of 3 members: NPAL1, NPAL2, and NPAL3, with highly conserved amino acid sequences. The *NPAL1* and *NPAL2* genes were also reported as *NIPA3* and *NIPA4* because of the high similarity between NIPA and NPAL proteins at the amino acid level and the typical domain structure of these proteins [Goytain et al., 2007, 2008]. Especially the presence of 9 transmembrane domains is characteristic for NIPA and NPAL proteins, and these transmembrane domains are highly conserved in different species [Chai et al., 2003]. The divergence of these genes is believed to be an early event in vertebrate evolution [Goytain et al., 2007], but to date very little is known about the expression and the function of the *NPAL* genes. However, it is well known that transmembrane-localized proteins are important for intercellular communication and for the proper development of many different species [Kopczynski et al., 1998]. Very recently, it was demonstrated that the level of NPAL1 and NPAL3 proteins increased in kidneys of mice which were maintained on magnesium-restricted diet; however, both proteins are not selective to Mg^{2+} ion transport [Goytain et al., 2008]. The first data about the human *NPAL3* gene derived from a shotgun DNA sequencing project [Andersson et al., 1996], and the complete *NPAL3* gene was identified on chromosome 1p36.12→p35.1 in the report from the human chromosome 1 sequencing project [Gregory et al., 2006]. The mouse *Npal3* sequence was already identified in a large cDNA library building and sequencing project [Bonaldo et al., 1996]. Nevertheless, to date nothing is known about the expression and function of NPAL3 proteins.

The high similarity between NPAL proteins and NIPA proteins prompted us to analyze the *Npal3* and *NPAL3* genes in more detail. Here, we present expression analyses of the mouse *Npal3* gene and its human homologue *NPAL3*. To elucidate the role of *Npal3* we have generated a knockout mouse line which was analysed in the comprehensive primary phenotypic screen of the German Mouse Clinic. The phenotypic analyses revealed altered behavior of *Npal3*$^{-/-}$ mice as well as an effect of the mutation on the immune system. Moreover, disruption of the *Npal3* gene was found to affect the lung function and resulted in increased IgE levels in mutant male mice. Thus, *Npal3* could serve as a candidate gene involved in atopic diseases.

Material and Methods

Data Base Searches and Computational Analysis

Nucleotide sequences and deduced protein sequences of mouse *Npal3* (Gene ID: 74552) and human *NPAL3* (Gene ID: 57185) were subjected to homology searches using the BLAST program [Altschul et al., 1990] in the public database NCBI (http://ncbi.nlm.nih.gov). Prediction of the protein molecular weight (MW) and isoelectric point (pI) was done using the Protein Calculator (http://www.scripps.edu/~cdputnam/protcalc.html). Putative structural and functional motifs were analyzed by PSORT II (http://psort.nibb.ac.jp/psort/helpwww2.html) and TMHMM (http://www.cbs.dtu.dk/services/TMHMM/) [Moller et al., 2001]. Multi sequence alignment was performed using the ClustalW program (http://align.genome.jp/). The cDNA sequence analysis was done by using the Wisconsin Package (GCG) version 11.1.

Northern Blot Analysis

Total RNA was extracted from different mouse tissues and from the brain of macaque *(Macaca mulatta)*, rat *(Rattus norvegicus)*, hamster (*Phodopus* sp.), and rooster *(Gallus gallus)* using the RNA now kit (Biomol, Hamburg, Germany) according to the manufacturer's recommendation. Subsequently, RNA samples (20 μg per lane) were fractionated on denaturing 1.5% MOPS/formaldehyde agarose gels [Hodge, 1994] and transferred onto Hybond N membranes (Amersham, Freiburg, Germany). For human expression analysis, commercially available human multiple tissue Northern blots (BD Biosciences Clontech, Heidelberg, Germany) were used. For hybridization a ^{32}P-labeled mouse *Npal3* cDNA clone (IMAGE998O241034) and a human *NPAL3* cDNA clone (IMAGp998A0674) from the German resource center (RZPD, Berlin, Germany) were used as probes, respectively. The filters were subsequently rehybridized with a ^{32}P-labeled *EEF-2* cDNA (Gene ID: 1938) [Rapp et al., 1989] or a human *ACTB* cDNA (Gene ID: 60) probe (IMAGp998L23787).

Reverse Transcription PCR Analysis

For reverse transcription (RT)-PCR, DNAse-I-treated total RNA from murine embryonic tissues was reverse-transcribed into cDNA at 42°C for 1 h using the Superscript reverse transcriptase system (Invitrogen) and the Oligo $dT_{12–18}$ oligonucleotide

according to the manufacturer's recommendations. An aliquot (1 μl) from a 1:10 dilution was subjected to 35 rounds of PCR with 0.5 units Taq DNA polymerase (Invitrogen). For expression analysis of the mouse *Npal3* gene primers JKSP6L (5′-GAC ATG GCT TCC AGT TCA CAC-3′) and JKT7L2 (5′-AGC CAC CAT GTC TTG GTC TTG-3′), generating a 326-bp product, were used.

For expression analysis of the human *NPAL3* gene in fetal tissues primers YLHF (5′-CGC AAG AAC TGG AAA ACA CAC-3′) and YKHR (5′-AAG TGC AAT GCT GAC CAC GAG-3′), generating a 385-bp fragment, were used on the Genefinder library (RZPD) as a template. To rule out template contamination in reaction components or DNA contamination in RNA samples a negative control without reverse transcriptase enzyme was performed simultaneously. The amplification profile involved 5 min at 95°C followed by 35 cycles of 1 min at 95°C, 1 min at 65°C, and 1 min at 72°C and finally 7 min at 72°C. To test the RNA quality $GAPDH_{for}$ (5′-CAT CAC CAT CTT CCA GGA GC-3′) and $GAPDH_{rev}$ (5′-ATG ACC TTG CCC ACA GC CTT-3′) primers, amplifying a 444-bp fragment of mouse or human *Gapdh/GAPDH,* were used.

Genomic Library Screening

Computer-spotted 129Sv mouse genomic cosmid library filters supplied by the RZPD were used for the identification of murine *Npal3* genomic clones. Screening of the cosmid library was performed according to the standard protocol supplied by the RZPD using the ^{32}P-labeled *Npal3* cDNA clone as a probe. The hybridization buffer contained 0.5 M phosphate buffer (pH 7.2), 7% SDS, 1 mM EDTA, and 100 μg/μl denatured salmon sperm DNA. Hybridization was carried out at 65°C overnight. Washing was performed with 25 mM phosphate buffer (pH 7.2) and 0.1% SDS. Filters were autoradiographed with intensifying screens at –80°C for 16 h. Two genomic clones, together containing the entire mouse *Npal3* gene including flanking regions, were isolated and characterized by restriction analysis and partial sequencing.

Chromosomal Localization by Fluorescence in situ Hybridization (FISH)

The DNA of the mouse *Npal3* genomic cosmid clone (MPMGc121G05246Q2, RZPD) was labeled with digoxigenin-11-dUTP by nick-translation and hybridized in situ to metaphases of the WMP-1 cell line [Zornig et al., 1995]. Signal detection via fluorescinated avidin (FITC-avidin) was performed as described [Lichter et al., 1988]. Chromosomes were counterstained with 4′,6-diamidino-2-phenylindole dihydrochloride (DAPI). Images of emitted light were captured separately by use of the DAPI and FITC filter set and subsequently merged and aligned.

Construction of the Npal3 *Gene Disruption Vector*

Two cosmid clones (MPMGc121G05246Q2 and MPMGc121J21285Q2, RZPD), containing the sequence of the mouse *Npal3* gene, were used for generation of the knockout construct. The 5′ part of the *Npal3* gene was generated upstream of the translation initiation site ATG in exon 2 by using the proofreading Easy-A® High-Fidelity PCR Cloning Enzyme (Stratagene, La Jolla, CA, USA) and cosmid DNA as a template. For directional cloning into the multiple cloning site of the pTKNeo vector [Rosahl et al., 1995] overhanging *Sal*I and *Cla*I restriction sites were introduced using the following oligonucleotides: Co93ForSal (5′-ACG CGT CGA CGT TCT TTG GTC AAA CTG AAT CGT C-3′) and Co93RevCla (5′-CCA TCG ATC CTG CCG GGC CAG GCT GGG CGC TG-3′), respectively. Using these primers for PCR a 3.0-kb genomic DNA fragment of the *Npal3* gene was amplified, subsequently cloned into the pGEM-T vector-system (Promega, Madison, USA), and completely sequenced. The *Sal*I and *Cla*I restricted 5′ part of the *Npal3* gene was then isolated and ligated into the *Sal*I and *Cla*I sites of the pTKNeo vector. Positive pTKNeo subclones containing the 3.0-kb 5′ gene fragment of *Npal3* were subsequently linearized by digestion with *Bam*HI and *Not*I, and a 15-kb-long 3′-*Bam*HI/*Not*I genomic DNA fragment, covering exon 9 of the *Npal3* gene, was ligated into the pTKNeo vector by using the Express-Ligation-System (BD Biosciences Clontech). The obtained *Npal3* gene targeting vector was linearized with *Not*I and electroporated into R1 ES cells [Wurst and Joyner, 1993]. ES cell colonies resistant to G418 (400 μg/μl) and ganciclovir (2 μM) were selected. Genomic DNA was extracted from selected ES cell clones, digested with *Bam*HI, electrophoresed, and blotted onto Hybond N membranes (Amersham). The filters were hybridized with a ^{32}P-labeled 479-bp-long *Bam*HI/*Hin*dIII genomic DNA fragment which was used as an external probe. Hybridization was carried out at 65°C overnight in Rapid hybridization buffer (Amersham) and 100 μg/μl denatured salmon sperm DNA. Filters were washed twice to final stringency at 0.2× SSC/0.1% SDS. Filters were autoradiographed with intensifying screens at –80°C for 16 h. ES cell clones carrying the disrupted *Npal3* allele were used for generation of chimeras. Male chimeras were mated to C57BL/6J and 129/Sv females, and the resulting F_1 offspring were genotyped by PCR analysis. For PCR genotyping the genomic DNA was extracted from mouse tails. PCR was carried out for 35 cycles using the following conditions: 30 s at 94°C, 30 s at 60°C, and 30 s at 72°C. The following primers were used to discriminate wildtype and mutant alleles: KOFor (5′-ATC AGA GGA CTC CTT TGG CTG-3′), KORev (5′-TGT AGG AGA AGG AGC CCT CGC-3′), and NeoRev (5′-CAG AGG TTA CGC AGT TTG TC-3′). The amplification products were analyzed on a 1.0% agarose gel. A 350-bp fragment of the mutant allele was amplified with primers KOFor and NeoRev, whereas primers KOFor and KORev amplified a 250-bp wildtype product. Heterozygous animals were crossed to obtain homozygous mutants.

Phenotype Analysis of Npal3$^{-/-}$ *Mice*

The German Mouse Clinic (GMC) provides an open access platform for standardized mouse phenotyping [Gailus-Durner et al., 2005]. For the screen 14 adult *Npal3*$^{-/-}$ females, 14 *Npal3*$^{-/-}$ males, 17 *Npal3*$^{+/+}$ control females, and 9 *Npal3*$^{+/+}$ control males were analysed. Animals were housed in cages with individually ventilating system, with food and water ad libitum and light adjusted to a 12h/12h light/dark period. Health monitoring was carried out by on-site examination of the sentinel mice (8-week-old male SPF Swiss mice) by certified laboratories according to the Federation of European Laboratory Animal Science Associations (FELASA) recommendation. In the clinical chemical, dysmorphology, neurology, eye, nociception, expression profiling, energy metabolism, and pathology screens no genotype-specific differences could be found. Significant differences were observed in the following screens: behavior, immunology, allergy, and lung function. Only these screens are reported in detail.

Behavioral Screen. The modified hole board test was carried out according to the procedures described by Ohl et al. [2001] to

analyze naïve mice at the age of 8 weeks. The apparatus consisted of a test arena (100×50 cm), in the middle of which a board (60×20×2 cm) was placed with 23 holes (1.5×0.5 cm) staggered in 3 lines with all holes covered by movable lids, thus representing the test arena as an open field. The area around the board was divided into 12 similarly sized quadrants by lines taped onto the floor of the box. Both box and board were made of dark grey PVC. All lids were closed before the start of a trial. For each trial a familiar object (metal cube) and an unfamiliar object (a blue plastic tube lid, similar in size to the metal cube) were placed into the test arena with a distance of 2 cm between them. The illumination levels were set at approximately 150 lux in the corners and 200 lux in the middle of the test arena. For testing, each animal was placed individually into the same corner of the test arena and allowed to explore for 5 min. The locomotor path was videotaped. The 2 objects were placed in the corner quadrant diametrical to the starting point. Data were analyzed by using the Observer 4.1 Software and the Ethovision 2.3 video-tracking system (Noldus, Wageningen, Germany). After each trial, the test arena was cleaned carefully.

Allergy Screen. 12-week-old mice were screened for alterations in plasma total IgE concentration. Blood samples were taken from animals by puncturing the retro-orbital plexus under ether anesthesia. Plasma IgE concentration was measured by isotype-specific sandwich ELISA technique with a lower detection limit of 1 ng/ml. The plates were read in a standard microplate reader at a wavelength of 450 nm. Total murine IgE data are reported in ng/ml, based on a standard curve of purified murine IgE [Alessandrini et al., 2001].

Immunological Screen. Peripheral blood leucocytes (PBLs) were isolated from 500 μl blood (please see above) by erythrocyte lysis with 0.17 M NH_4Cl-Tris buffer (pH 7.45) directly in 96-well microtiter plates. After subsequent washing with FACS staining buffer (PBS, 0.5% BSA, 0.02% sodium azide, pH 7.45), PBLs were incubated for 20 min with 1 μM ethidium monazide bromide (EMA, Molecular Probes, Netherlands) and Fc block (clone 2.4G2, PharMingen, San Diego, USA). EMA bound to the DNA of dead cells was photocrosslinked. Cells were then stained with fluorescence-conjugated monoclonal antibodies (PharMingen). The following main cell populations were analyzed: B cells ($CD19^+$ clone 1D3), B1 B cells ($CD19^+CD5^+$, clone 53-7.3), B2 B cells ($CD19^+CD5^-$), T cells ($CD3^+$, clone 145-2C11), $CD4^+$ T cells (clone RM4-5), $CD8^+$ T cells (CD8α, clone 53.6-7; CD8β, clone H35-17.2), γ/δδT cells (clone GL3), granulocytes ($Gr\text{-}1^+$, clone RB6-8C5), and NK cells ($CD49b^+$, clone DX5). We also analyzed additional subpopulations based on the following surface antigens: IgD (clone 11-26c.2a), B220 (clone RA3-6B2), CD11b (clone M1/70), CD103 (clone 2E7), CD25 (clone PC61), CD62L (clone MEL-14), CD45RA (clone 14.8), Ly-6C (clone AL-21), and CD44 (clone IM7). Data were acquired on a FACS Calibur (BectonDickinson, San Diego, USA) and were analyzed using FlowJo software (Tree-Star Inc, USA). All samples were acquired until a total number of 25,000 cells was reached. The plasma level of IgM, IgG_1, IgG_{2a}, IgG_{2b}, IgG_3, and IgA was determined by standard sandwich ELISAs using goat anti-mouse alkaline phosphatase (AP) conjugated antibodies (SouthernBiotech, Birmingham, USA). The presence of rheumatoid factor and anti-DNA antibodies was evaluated by indirect ELISA with rabbit IgG and calf thymus DNA (Sigma-Aldrich, Steinheim, Germany), respectively, as antigens and AP-conjugated goat anti-mouse secondary antibody (Sigma-Aldrich). Serum samples from MRL/MpJ-$Tnfrsf6^{lpr}$ mice (Jackson Laboratory, Bar Harbor, USA) were used as positive controls in the autoantibody assays.

Lung Function Screen. The whole body plethysmography (Buxco Research Systems, Sharon, USA) was used to assess breathing patterns in unrestrained animals aged 16 weeks [Drorbaugh and Fenn, 1955] by measuring the pressure changes which arise from inspiratory and expiratory temperature and humidity fluctuation during breathing. Calibration of the system allows to transform these pressure swings into flow and volume signals so that automated data analysis provides tidal volumes (TV), respiratory rates (f), minute ventilation (MV), inspiratory and expiratory times (Ti, Te), as well as peak expiratory flow rates (PIF, PEF). Data were collected at 10-second intervals. Measurements were always performed between 8 a.m. and 11 a.m. to account for potential diurnal variation in breathing. The system was setup in a quiet room with constant temperature and humidity. After placing the animal into the chamber data recording started immediately and was continued during 40 min. Primarily, mice were stressed so that the respiratory rate was highest at the beginning. Usually after 5 min the animals slightly reduced their respiratory rate and began to explore the chamber – this was called 'phase of activity'. Later activity was more and more interrupted by phases of rest or even short periods of snoozing – 'resting phase'. Some of the animals even went to a 'phase of sleep', which resulted in a further marked decrease in respiratory rate. The frequency histogram of the respiratory rates was determined for each individual animal and breathing was analysed for the above mentioned parameters during the phase of activity and rest. In addition to the directly recorded parameters, mean inspiratory and expiratory flow rates (MEF and MIF) were calculated offline from the ratio of tidal volume and the respective time interval. The relative duration of inspiration (Ti/TT) was determined from the ratio of inspiratory time to total time required for the breathing cycle. Specific tidal volumes and minute ventilations (sTV, sMV) were calculated by relating the absolute values to the body weight of the animal. Furthermore, the mean of all breathing frequencies (mean_f) measured during the 40-min period was calculated as a rough and ready parameter to assess whether the duration of rest and activity was similar in both mouse strains.

Statistical Analysis

Data of males and females were analysed separately comparing mutant and control data using the Student t test using the Statgraphics (Statistical Graphics Corporation, Rockville MD) or SPSS (SPSS Inc., Chicago, Ill., USA) software. Tables summarizing the data show mean ± standard error of the mean. The chosen level of significance was $p < 0.05$.

Results

The Npal3 *Gene Is Highly Conserved during Evolution and Encodes a Putative Transmembrane Protein*

Sequence analysis in the NCBI GenBank database demonstrated that the mouse *Npal3* cDNA consists of a 355-bp-long 5′-UTR, an open reading frame (ORF) of 1,230 bp coding for a putative protein of 410 amino acids

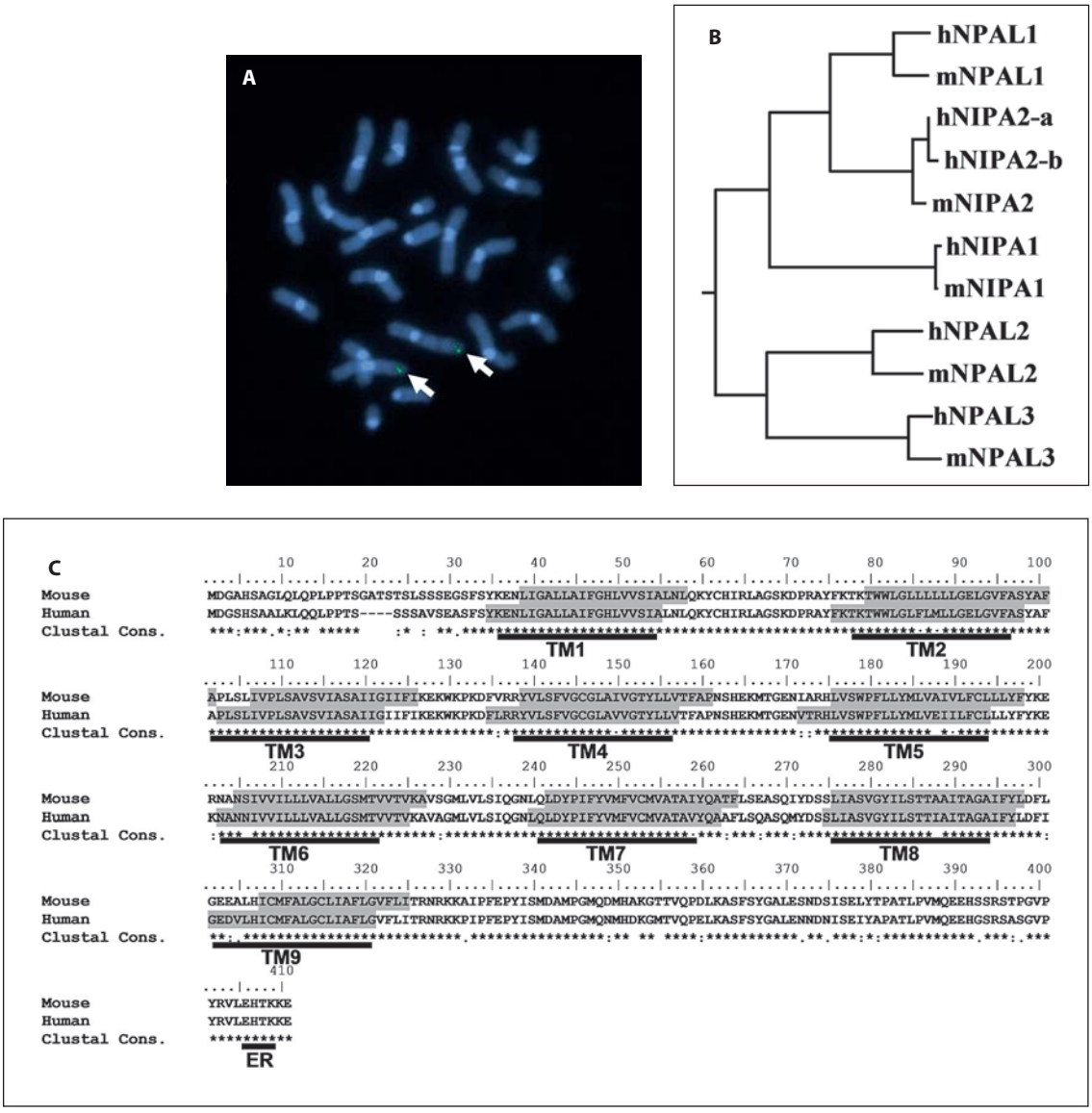

Fig. 1. A Chromosomal localization of *Npal3* using fluorescence in situ hybridization (FISH) on metaphase chromosomes from WMP-1 murine cells with a probe specific for *Npal3*. The arrows point to the specific signals of the mouse *Npal3* gene on chromosome 4, region D3. **B** Phylogenetic tree constructed from multiple alignment of mouse (m) and human (h) NIPA/NPAL proteins. The letters a and b indicate 2 isoforms of the human NIPA2 protein. The tree was generated by using the GCG software package. **C** ClustalW alignment of human and mouse NPAL3, highly conserved amino acids are indicated by asterisks. The amino acids of the 9 predicted transmembrane domains (TM) using the TMHMM software are marked in gray and are underlined. The endoplasmic reticulum (ER) retention-like motif at the C-terminal end is indicated. Clustal Cons. – the ClustalW consensus sequence is marked by asterisks.

in length (Acc. No.: NP_083271), and a 3′-UTR of 857 bp in size. The *Npal3* gene contains 12 exons and spans a genomic segment of 46 kb on mouse chromosome 4D3. To further analyze this so far non-characterized *Npal3* gene, a genomic cosmid clone MPMGc121G05246Q2 for *Npal3* was isolated and used as a probe for chromosomal localization using fluorescent in situ hybridization (FISH). This analysis confirmed the predicted chromosomal localization of the *Npal3* gene on mouse chromosome 4D3 (fig. 1A).

The phylogenetic tree of the mouse and human NIPA/NPAL protein family, generated with the GCG software

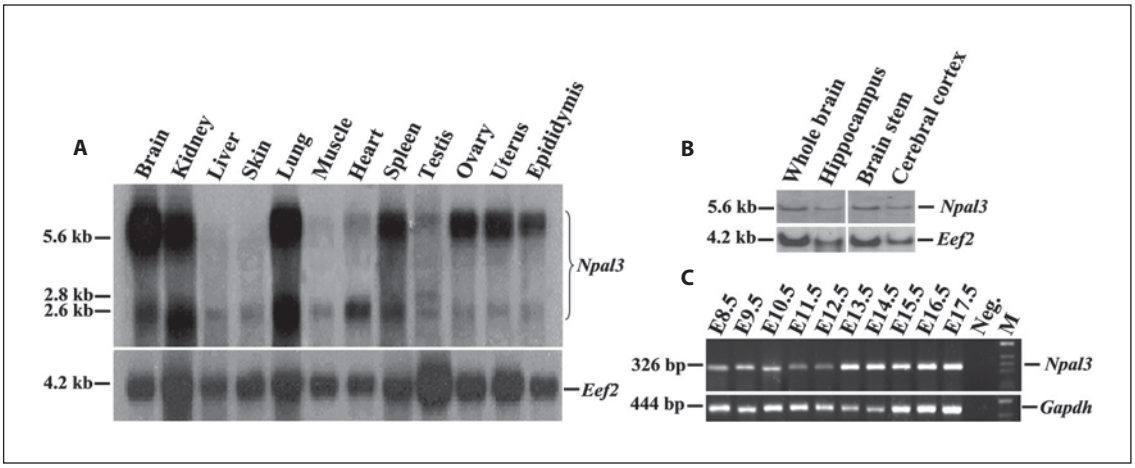

Fig. 2. Expression analyses of mouse *Npal3* in murine postnatal tissues and during embryonic development. **A** Northern blot analysis of RNA derived from different postnatal mouse tissues revealed an ubiquitous expression of the *Npal3* gene in all tissues analyzed. Besides 2 ubiquitous *Npal3* transcripts (5.6 and 2.6 kb), an additional 2.8-kb *Npal3* transcript was observed exclusively in the testis. To verify the integrity of the RNA samples, all membranes were rehybridized with a human elongation factor-2 *(Eef2)* cDNA probe. **B** Northern blot analysis of mouse *Npal3* expression on RNA samples isolated from different parts of the mouse brain. A *Npal3* transcript was detected in the hippocampus, brain stem, and cerebral cortex. **C** Analysis of *Npal3* expression during embryonic development was performed using RT-PCR and *Npal3*-specific primers JKSP6L and JKT7L2. Expression of *Npal3* was detectable in all stages analyzed, starting from day 8.5 post coitum. The cDNA quality was verified using *Gapdh*-specific primers.

package, is shown in figure 1B. The NPAL1 and NIPA2 proteins show the highest relationship within this protein family, and NPAL1 and NIPA2 display a higher similarity at the amino acid level (68–70%) as compared to the NIPA1 protein. The NPAL2 and NPAL3 proteins build a separate branch, and these proteins exhibit 39% identity at the amino acid level. The alignment of NIPA/NPAL proteins from 13 different species resembled the same evolutionary relationship on the dendrogram (supplementary fig. 1; for online supplementary material, see www.karger.com/doi/000230003).

The human and mouse NPAL3 proteins share 88% similarity (fig. 1C), and the cDNA sequences between mouse *Npal3* and human *NPAL3* are also highly conserved with 85% homology at the nucleotide level. The complete *NPAL3* cDNA is 5,297 bp in size; the ORF of 1,218 bp encodes a putative 406-amino-acid-long protein and is flanked by a 331-bp-long 5′-UTR and a 804-bp-long 3′-UTR, respectively. The human *NPAL3* gene contains 12 exons and spans a region of 57 kb on chromosome 1p36.12→p35.1.

To predict putative domains in NPAL3 proteins and to elucidate their function the PSORTII program was used. This computational search revealed 9 transmembrane domains and an ER membrane retention signal-like motif (HTKK) at the C-terminus of NPAL3 proteins. To verify this finding the NPAL3 amino acid sequence was subjected to the TMHMM program, especially designed to detect transmembrane helices in proteins. This analysis confirmed the presence of 9 transmembrane domains in the NPAL3 protein sequence, and moreover, this domain pattern is highly conserved between mouse and human (fig. 1C, gray boxes). Besides the transmembrane domains, these proteins seem to consist of an N-terminal extracellular domain and a C-terminal cytoplasmatic domain. Using the protein calculator program, the theoretical molecular weight (MW = 44.7 kDa) and the isoelectric point (pI = 7.98) of the NPAL3 protein were calculated.

Expression of Mouse Npal3 *and Human* NPAL3 *Genes*

To analyze the expression profile of the mouse *Npal3* gene, total RNA samples isolated from different adult mouse tissues were hybridized with a ^{32}P-labeled *Npal3* cDNA probe. Two transcripts, 5.6 kb and 2.6 kb in size, were detected in all tissues analyzed (fig. 2A). In the testis an additional 2.8-kb transcript was observed. The strongest *Npal3* gene expression was found in the brain, and strong signals were also detected in kidney, lung, and

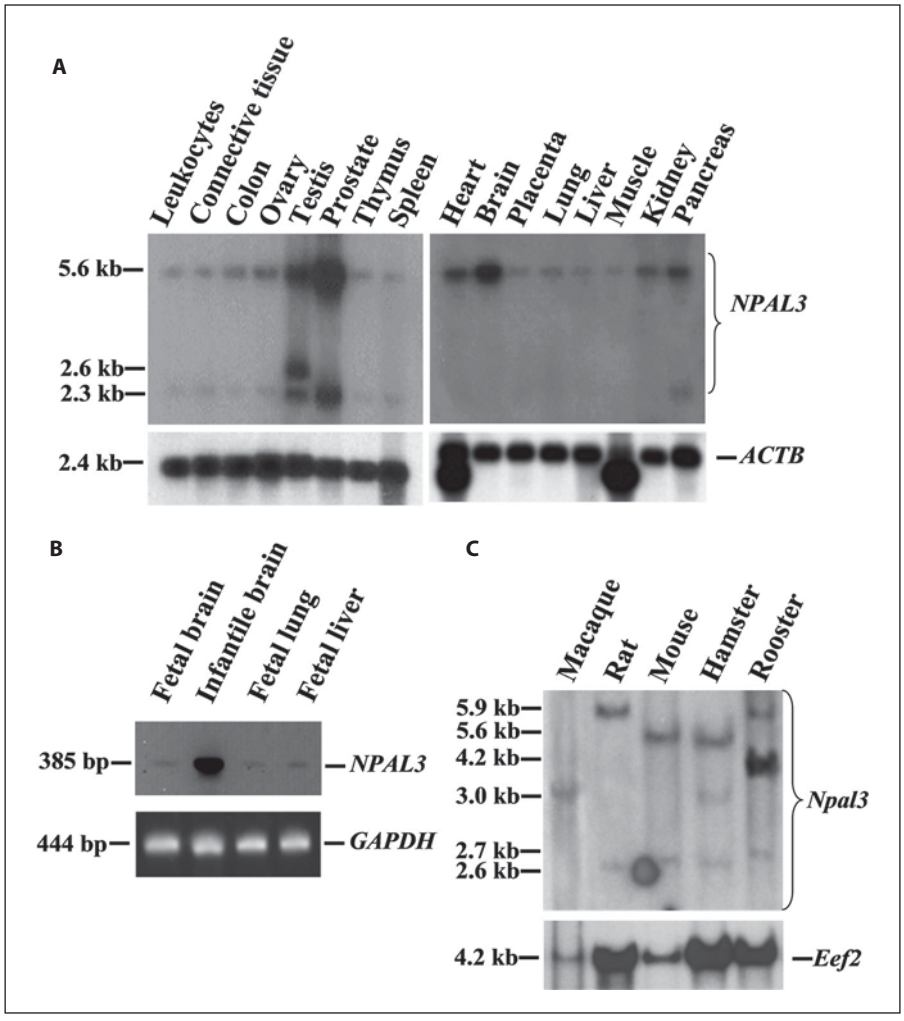

Fig. 3. Expression analyses of the human *NPAL3* gene. **A** Northern blot analysis using human *NPAL3* cDNA as a probe demonstrated a ubiquitous expression of this gene in all tissues analyzed. Two *NPAL3* mRNA fragments of 5.6 and 2.3 kb were identified in different tissues, whereas in the testis an additional 2.6-kb transcript was detected. The RNA quality was verified using a human beta-actin cDNA as a probe (*ACTB*). **B** To study the expression of the *NPAL3* gene in different human fetal tissues and in infantile brain a Genefinder cDNA library was analyzed using PCR. A 385-bp-long *NPAL3*-specific product could be amplified in all tissues, and the strongest expression was detected in infantile brain. The cDNA quality was tested with human *GAPDH*-specific primers. **C** Mouse *Npal3* cDNA was used as a probe in a Northern blot experiment on RNA samples isolated from the brains of different species. In the RNA isolated from macaque brain a single 3.0-kb-long transcript was detected, in rat and mouse 2 isoforms, and in hamster and rooster 3 isoforms of *Npal3* could be observed, respectively. The RNA quality was checked by re-hybridization with a human elongation factor-2 *(Eef2)* cDNA as a probe.

spleen. The weakest signals appeared in liver, skin, and muscle. Next, *Npal3* gene expression was analyzed in different parts of the mouse brain. The Northern blot experiment revealed that the *Npal3* gene is expressed in the hippocampus, brain stem, and cerebral cortex (fig. 2B). Quantity and integrity of RNA samples were demonstrated by re-hybridizing the blots with an *Eef2* cDNA probe. In order to study the expression of the *Npal3* gene during mouse embryonic development RT-PCR analysis was used. *Npal3* expression was detected in all embryonic developmental stages analyzed (fig. 2C). Finally, RNA quality of the samples was checked using RT-PCR with *Gapdh*-specific primers.

The IMAGp998A0674 cDNA clone was used to generate a human probe for expression analysis of the *NPAL3* gene. Human multiple tissue Northern blots were hybridized with a ^{32}P-labeled *NPAL3*-specific cDNA probe, and 2 transcripts (5.6 kb and 2.3 kb in size) were detected in all tissues and cells analyzed (fig. 3A). In the human testis an additional 2.6-kb *NPAL3* signal was detected, which is comparable to the situation observed in the mouse testis. In human tissues the strongest *NPAL3* gene expression was detected in the prostate, followed by brain and testis. The weakest *NPAL3* expression was observed in liver and muscle. RNA quality and integrity was checked using a human *ACTB* cDNA as a probe. Furthermore, the 'Genefinder' cDNA library from the RZPD was used to analyze the expression of the *NPAL3* gene in fetal human tissues and infantile brain. A 385-bp-long *NPAL3*-specific PCR product could be amplified of cDNA derived from fetal and infantile brain, fetal lung, and liver (fig. 3B). The cDNA quality of the samples was verified using PCR with *GAPDH*-specific primers.

As already mentioned above human NPAL3 and mouse Npal3 share high similarities at the amino acid level. To determine whether the *Npal3* gene is conserved in diverse vertebrates, databases TBLASTN and ENSEMBL were searched with conserved NPAL3 amino acid queries. These database searches demonstrated that the NPAL3 protein is highly conserved within 13 species from 8 orders of vertebrates including: Primata (orangutan, crab-eating macaque, rhesus monkey, chimpanzee and human), Rodentia (rat and mouse), Perissodactyla (horse), Carnivora (dog), Monotremata (platypus), Didelphimorphia (gray short-tailed opossum), Galliformes (chicken), and Anura (western clawed frog). In supplementary figure 2 the ClustalW multiple global alignment of NPAL3 is presented. Next, we have used a mouse *Npal3* cDNA probe in a Northern blot experiment to analyze the expression of this gene in the brain of different mammals and from rooster. In the brain from macaque 1 transcript (3.0 kb) was detected, in rat brain 2 transcripts (5.9 and 2.6 kb) were present, and in the brain from hamster and rooster 3 signals were obtained (5.6, 3.0, 2.6 and 5.9, 4.2, 2.7 kb, respectively, fig. 3C). To prove RNA quality and integrity the membrane was re-hybridized using an *Eef2* cDNA as a probe. Taken together, our results demonstrate that mouse *Npal3* and human *NPAL3* are highly conserved genes which are ubiquitously expressed in mouse and human tissues.

Targeted Disruption of the Npal3 *Gene in Mice*

Using a gene targeting approach we have generated homozygous *Npal3*$^{-/-}$ mice to elucidate the functional role of the *Npal3* gene. The mouse *Npal3* gene was disrupted in ES cells by homologous recombination using a replacement-targeting vector containing pTKNeo and thymidine kinase expression cassettes. The neomycin (Neo) cassette replaces part of exon 2 containing the start codon ATG as well as exons 3 to 8 of the *Npal3* gene (fig. 4A). We obtained one correctly targeted ES cell clone which was identified using Southern blot analysis with an external probe located upstream of the 5′ flanking region of the targeting construct (fig. 4B). The external probe detected the wild type allele as a 3.9-kb fragment and the recombinant allele as an 8.6-kb fragment in genomic ES cell DNA digested with the *Bam*HI restriction enzyme. The ES cells from this clone were injected into C57BL/6J blastocysts to generate chimeric mice. Male chimeric mice transmitting the targeted mutation into the germ line were bred with female mice from C57BL/6J and 129X1/SvJ strains to establish the *Npal3* knockout model in 2 different genetic backgrounds. Heterozygous animals were identified by PCR analysis of DNA obtained from mouse tails and were intercrossed to generate homozygous mice in the respective genetic backgrounds. PCR analysis of the F_2 progeny revealed the normal Mendelian ratio of wildtype, heterozygous, and homozygous animals, respectively (fig. 4C). In homozygous mutant mice the lack of *Npal3* gene expression in brain was confirmed by Northern blot analysis using a *Npal3*-specific cDNA as a hybridization probe (fig. 4D). The quality and integrity of the RNA samples was visualized by ethidium bromide staining.

Phenotypical Analyses of Npal3 *Knockout Mice*

Homozygous animals grew normal and were fertile without any obvious phenotype. The morphology, anatomy, and histology analyses of brain, testis, and other organs did not reveal any abnormalities (data not shown).

In order to analyze if the brain function was affected in mutant mice the modified hole board test was used. This test allows the comprehensive analysis of a range of parameters known to be indicative of behavioral dimensions such as locomotor activity, exploratory behavior, arousal, emotionality, memory, and social affinity [Ohl et al., 2001]. Behavioral analysis of spontaneous activity in the modified hole board as a novel environment revealed increased frequency for group contacts and a tendency towards reduced latency to first group contact in *Npal3*$^{-/-}$ females (table 1). The time spent in social contact did not significantly differ between mutant and control animals (table 1, total duration). In the hole exploration test *Npal3*$^{-/-}$ males started the hole exploration earlier than control males, but hole exploration frequency remained unchanged (table 1). There were no genotype effects in any other observed parameters (supplementary table 1).

The immunology screen was set up to conduct a broad immunological phenotyping of the *Npal3*$^{-/-}$ mutant line. This analysis revealed minor, but significant differences affecting NK cell number (table 2, CD49b^{+}), which was decreased in mutants. In addition, changes in the levels of IgM, IgG_{2a}, and IgA were observed (table 2). In all other analyzed parameters no significant differences were observed (supplementary table 2).

Next, 10 *Npal3*$^{-/-}$ males and 11 *Npal3*$^{-/-}$ females were analyzed for the level of total IgE. As a control 15 *Npal3*$^{+/+}$ males and 14 *Npal3*$^{+/+}$ females were used. This screen clearly demonstrated a higher concentration of IgE in mutant males in comparison to control males (298 ± 39 vs. 168 ± 12.7, respectively, $p < 0.02$). In mutant females

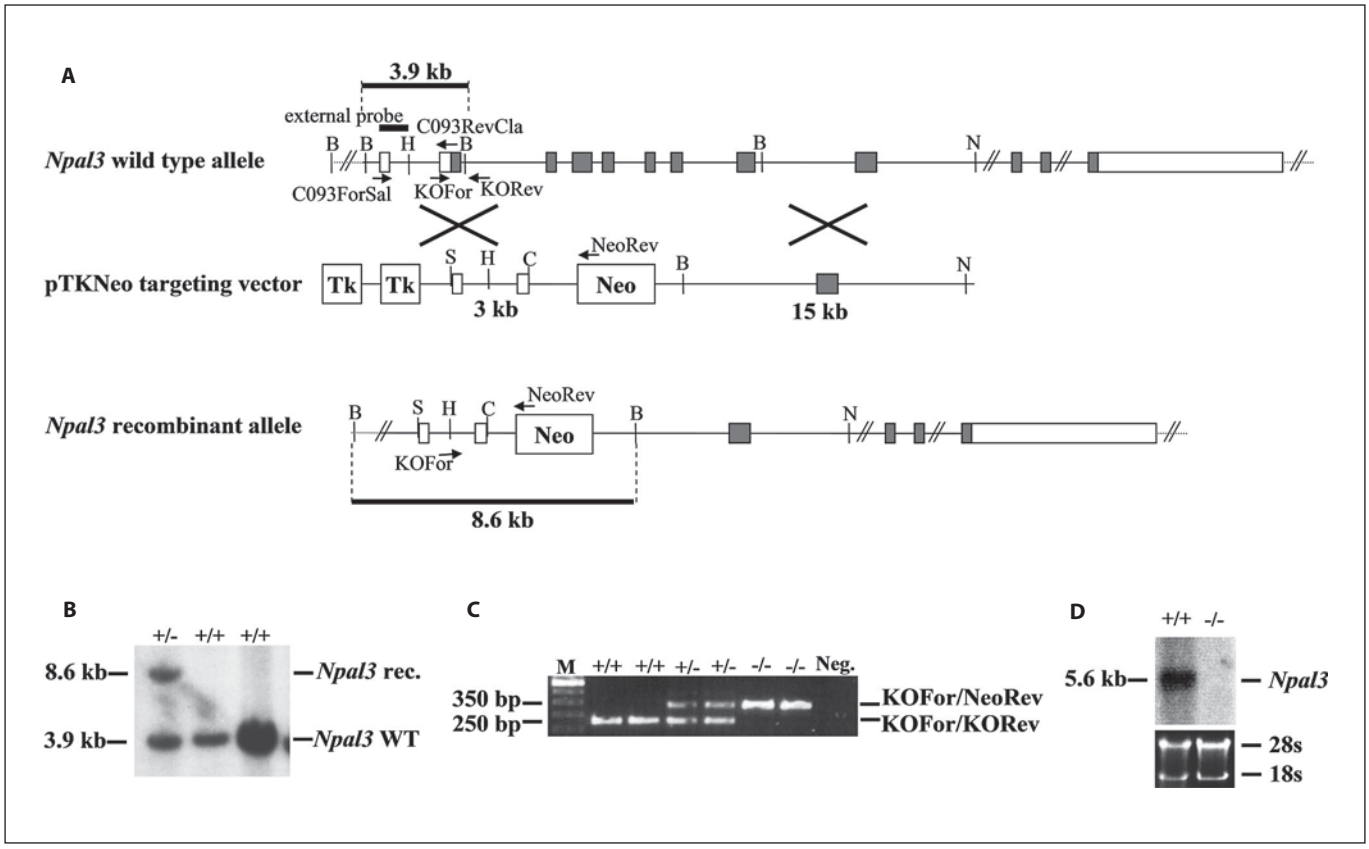

Fig. 4. Targeted disruption of the mouse *Npal3* gene. **A** Structure of the wild type and recombinant *Npal3* alleles are shown, relevant restriction sites (B, *Bam*HI; C, *Cla*I; H, *Hin*dIII; N, *Not*I; S, *Sal*I) and applied primers (C093ForSal, C093RevCla, KOFor, KORev, and NeoRev) are given. The knockout strategy was designed to replace part of exon 2 including the start codon ATG together with exons 3 to 8 of the *Npal3* gene with the *pgk-neo* cassette (Neo). A 3.0-kb-long genomic *Sal*I/*Cla*I *Npal3* fragment was generated by PCR using primers C093ForSal and C093RevCla. The wild type sequence of the complete *Npal3* fragment was verified by sequencing and cloned into the *Sal*I/*Cla*I sites of the pTKNeo vector. A 15-kb-long genomic *Bam*HI/*Not*I *Npal3* fragment was isolated from a cosmid clone and subcloned into the *Bam*HI/*Not*I sites of the pTKNeo vector. Tk, thymidine kinase cassette, gray boxes represent the ORF of the *Npal3* gene (from the start codon ATG in exon 2 to the stop codon TGA in exon 12). **B** Southern blot analyses to identify recombinant ES cell clones. Genomic DNA from ES cell clones was digested with *Bam*HI. Hybridization with a ^{32}P-labeled external probe shows a 3.9-kb band for the wild type *Npal3* allele (*Npal3* WT) and a 8.6-kb band for the recombinant *Npal3* allele (*Npal3* rec.) in one ES cell clone. **C** Genotyping of F_2 progeny by PCR using genomic DNA isolated from mouse tails and primers KOFor, KORev, and NeoRev. The wild type *Npal3* allele yields a PCR product of 250 bp and the mutated *Npal3* allele generates a 350-bp product. +/+: wild-type, +/–: heterozygous null, –/–: homozygous null. **D** Northern blot analysis of total RNA isolated from brain of *Npal3*$^{+/+}$ and *Npal3*$^{-/-}$ mice using *Npal3* cDNA as a probe. *Npal3* transcripts were observed in *Npal3*$^{+/+}$ but not in *Npal3*$^{-/-}$ mice (upper panel). RNA integrity and quantity was monitored by ethidium bromide staining (lower panel).

no significant difference could be observed (*Npal3*$^{-/-}$: 394 ± 64.4, *Npal3*$^{+/+}$: 380 ± 58.2).

The lung function screen was performed to elucidate the spontaneous breathing patterns during the time of rest and activity in *Npal3*$^{-/-}$ mice. Similar to the allergy screen described above this analysis demonstrated that only male mutants are affected but females remained without any changes (table 3). Mutant males used larger tidal volumes and little elevated respiratory rates during rest and activity; therefore, ventilation as well as specific tidal volumes and minute ventilation were significantly increased. The difference in flow rates – PEF and MEF during rest and MEF during activity – correlate to the differences in tidal volume. All measured parameters are given in supplementary table 3.

Table 1. Behavioral analysis in the modified hole board test

Parameter	*Npal3*$^{+/+}$		*Npal3*$^{-/-}$		Male p	Female p
	male (n = 10)	female (n = 15)	male (n = 8)	female (n = 15)		
Group contact (frequency)	12.40 ± 1.24	11.33 ± 1.24	14.00 ± 1.51	16.47 ± 1.16	n. s.	p < 0.01
Group contact (latency)	20.96 ± 5.65	45.45 ± 18.53	27.31 ± 5.82	19.03 ± 4.66	n. s.	p = 0.05
Group contact (total duration %)	21.76 ± 3.02	29.81 ± 3.7	25.36 ± 3.99	38.37 ± 4.1	n. s.	n. s.
Hole exploration (frequency)	25.8 ± 2.9	23.6 ± 3.35	19.5 ± 5.1	19.0 ± 3.39	n. s.	n. s.
Hole exploration (latency)	41.29 ± 15.64	24.33 ± 5.06	11.29 ± 3.33	75.79 ± 26.18	p < 0.05	n. s.

The data is given as a mean ± standard deviation. For the significant differences the p value is given.
n = Number of tested animals, n. s. = not significant.

Table 2. Immunology screen

Parameter	*Npal3*$^{+/+}$		*Npal3*$^{-/-}$		Male p	Female p
	male (n = 10)	female (n = 15)	male (n = 14)	female (n = 15)		
CD49b^{+}, %	11.3 ± 0.8	10.3 ± 1.0	8.5 ± 0.7	6.5 ± 0.7	p < 0.02	p < 0.01
IgG_{2a}, μg/ml	NA	995.4 ± 126	NA	1,603.5 ± 173	NA	p < 0.05
IgM, μg/ml	692.8 ± 67.1	515.1 ± 39.0	492.3 ± 66.2	657.7 ± 47.3	p < 0.05	p < 0.05
IgA, μg/ml	30.7 ± 6.0	166.1 ± 28.2	55.7 ± 9.7	117.2 ± 18.5	p < 0.05	n. s.

The data is given as a mean ± standard deviation. For the significant differences the p value is given.
n = Number of tested animals, NA = not analyzed, n. s. = not significant.

Table 3. Spontaneous breathing pattern during the time of rest and activity

Parameter	*Npal3*$^{+/+}$		*Npal3*$^{-/-}$		Male p	Female p
	male (n = 10)	female (n = 15)	male (n = 8)	female (n = 15)		
Rest						
sTV, μg/g	9.3 ± 0.3	11.2 ± 0.7	11.6 ± 0.3	10.7 ± 0.2	p < 0.01	n. s.
MV, ml/min	70.5 ± 4.0	81.3 ± 4.7	91.1 ± 4.0	71.1 ± 3.2	p < 0.01	n. s.
sMV, ml/min/g	2.4 ± 0.1	3.6 ± 0.2	3.5 ± 0.3	3.2 ± 0.1	p < 0.01	n. s.
PEF, ml/s	3.5 ± 0.3	3.9 ± 0.3	4.5 ± 0.2	3.2 ± 0.3	p < 0.02	n. s.
MEF, ml/s	1.8 ± 0.1	2.0 ± 0.1	2.4 ± 0.1	1.8 ± 0.1	p < 0.02	n. s.
Activity						
TV, ml	0.25 ± 0.01	0.25 ± 0.01	0.29 ± 0.01	0.24 ± 0.01	p < 0.02	n. s.
sTV, μl/g	8.5 ± 0.2	10.9 ± 0.6	11.2 ± 0.4	10.5 ± 0.3	p < 0.01	n. s.
MV, ml/min	101.0 ± 2.6	109.3 ± 6	123.5 ± 5.5	101.1 ± 5.7	p < 0.02	n. s.
sMV, ml/min/g	3.4 ± 0.1	4.8 ± 0.3	4.8 ± 0.3	4.5 ± 0.2	p < 0.01	n. s.
MEF, ml/s	2.6 ± 0.1	2.8 ± 0.1	3.3 ± 0.1	2.6 ± 0.1	p < 0.01	n. s.

The data is given as a mean ± standard deviation. For the significant differences the p value is given.
MEF = Expiratory flow rate, MV = minute ventilation, n = number of tested animals, NA = not analyzed, n. s. = not significant, PEF = peak expiratory flow rate, sMV = specific minute ventilation, sTV = specific tidal volumes, TV = tidal volume.

Discussion

The human *NPAL3* sequence was first identified in a sequencing approach [Andersson et al., 1996], but to date nothing is known about the expression or function of this gene. Here we could demonstrate that the mouse *Npal3* gene maps to chromosome 4D3 and that the *NPAL3* gene is localized in the syntenic region on human chromosome 1p36.12→p35.1. Both genes encode putative proteins containing 9 predicted transmembrane domains, and NPAL proteins are highly conserved during evolution. We could also show that mouse *Npal3* and human *NPAL3* genes are ubiquitously expressed in adult and fetal tissues. To elucidate the function of the *Npal3* gene, a knockout mouse model was generated. In *Npal3* mutant mice no obvious phenotype was observed, and therefore, $Npal3^{-/-}$ mice were analysed in the standardized comprehensive primary phenotypic screen [Gailus-Durner et al., 2005] of the German Mouse Clinic (GMC). This screen revealed that disruption of the *Npal3* gene leads to an altered function of both the nervous and immunological system in mutant male and female mice. Moreover, disruption of the *Npal3* gene also affected the lung function and resulted in an increased IgE level in $Npal3^{-/-}$ males.

The predicted chromosomal localization of the mouse *Npal3* could be confirmed by FISH. In both mouse and human *Npal3/NPAL3* genes the flanking sequences of the putative start codon ATG follow the Kozak prerequisites for a functional translation start codon [Kozak, 1999]. Furthermore, both *Npal3/NPAL3* sequences contain putative polyadenylation signals in the 3′-UTR, and both genes are expressed in adult and fetal tissues. The ubiquitous expression is in agreement with the UniGene data base (http://www.ncbi.nlm.nih.gov/UniGene) where 219 known *Npal3* cDNA clones are presented from a wide variety of tissues. In addition, by searching the Mouse Genome Informatics database (http://www.informatics.jax.org/), we could identify 58 *Npal3*-specific cDNA clones isolated from different pre- and postnatal mouse tissues. Moreover, expression of the *Npal3* gene was also observed in mouse spinal cord using the in situ hybridization technique. This data is available at the website of the Allen Institute for Brain Science (http://mouse.brain-map.org/). Downstream and upstream of *NPAL3/Npal3* the following genes are located: *GRHL3*, *IL28RA*, *IL22RA1*, *MYOM3, RCAN3, SRRM1, CLIC4,* and *RUNX3*. These genes are present in the syntenic region on both mouse and human chromosomes. Using mouse *Npal3* cDNA as a probe we could also detect *Npal3* transcripts in RNA from brain of different species, and moreover, the NPAL3 protein sequence is highly conserved. Taken together, all these observations suggest that human *NPAL3* and mouse *Npal3* encode functional proteins and that these proteins could play an important role in different cellular processes.

NPAL proteins display a similar structure comparable with NIPA proteins, and therefore, NPAL proteins could also play a similar role in molecular and cellular function. Recently, it was demonstrated that the *Drosophila* homologue *(Spic)* of human *NIPA1* is widely expressed and that this protein is localized on early endosomes [Wang et al., 2007]. In the present study we could demonstrate that mouse *Npal3* and human *NPAL3* are also ubiquitously expressed and both code for proteins containing 9 transmembrane domains and an ER membrane retention signal-like motif. Our model of the NPAL3 protein obtained by using the TMHMM program is very similar to the NIPA1 model in which also 9 transmembrane domains were identified [Goytain et al., 2007]. Thus, it can be speculated that the NPAL3 proteins are also localized in the cellular membrane system.

In the present study several mouse and human tissues were analyzed for *Npal3/NPAL3* expression studies, and always transcripts with different sizes were detected. Using the GCG software alternative polyadenylation signals were detected in the 3′-UTRs of both mouse and human *Npal3/NPAL3* genes. In the 3′-UTR of the human *NPAL3* gene 3 typical (AATAAA) and 11 untypical (AAGAAA, TCTGAA, ATTAAA, TCTAAA, CTTAAA, TACAAA) polyadenylation signals were found. In the 3′-UTR of the mouse *Npal3* gene 7 untypical (TCTGAA, GCAAAA, ATTAAA, TACAAA) polyadenylation signals could be identified. Previously, all these different signals were demonstrated to be utilized for polyadenylation [Meijer et al., 1987; Oyen et al., 1990; Wallace et al., 1999]. In the human *NPAL3* sequence the presence of the conserved polyadenylation signal AATAAA at nucleotide position 2896 after the stop codon TGA and of TCTAAA at position 404 after the TGA could explain the existence of transcripts 5.6 and 2.3 kb in size, respectively (fig. 5). In the mouse the modified polyadenylation signal ATTAAA at nucleotide position 3460 after the stop codon TGA and the GCAAAA signal at position 355 might be responsible for the presence of the 2 transcripts with 5.6 and 2.6 kb, respectively (fig. 5). It is worth noting that different polyadenylation signals were also described for members of the *NIPA* gene family. The *Nipa1*/*NIPA1* genes from mouse and human as well as the mouse *Nipa2* gene were shown to express 2 transcripts with different sizes as the result of 2 different polyadenylation signals in

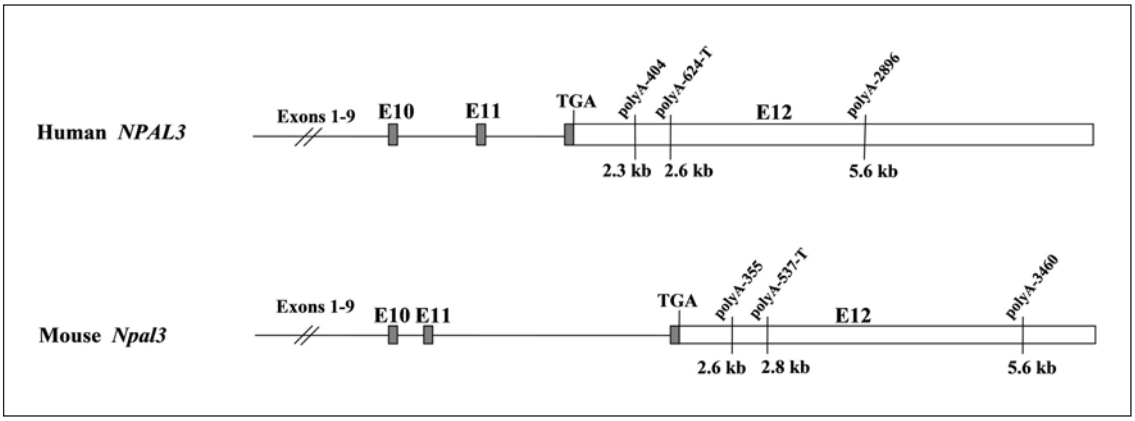

Fig. 5. Localization of alternative polyadenylation signals in human *NPAL3* and mouse *Npal3* genes. In the respective 3′-UTRs (exon 12) of both human and mouse *NPAL3*/*Npal3* genes alternative polyadenylation signals are marked at the nucleotide position after the stop codon TGA. In *NPAL3* the putative polyadenylation signal (polyA-2896) at position 2896 after the stop codon TGA could explain the existence of the 5.6-kb-long *NPAL3* transcript, at position 404 (polyA-404) after the stop codon the 2.3-kb-long isoform, and at position 624 (polyA-624-T) the 2.6-kb-long testis-specific *NPAL3* transcript. In the mouse *Npal3* gene the putative polyadenylation signals at position 3460 (polyA-3460), at 355 (polyA-355), and at 537 (polyA-537-T) correspond to the 5.6-kb, 2.6-kb, and 2.8-kb (testis-specific) long *Npal3* transcripts, respectively.

their respective 3′-UTRs [Chai et al., 2003; Rainier et al., 2003].

An additional polyadenylation signal TCTGAA at nucleotide position 624 after the stop codon in the human *NPAL3* gene and at position 537 after the stop codon in the mouse *Npal3* gene could explain the existence of the 2.6-kb (human) and 2.8-kb (mouse) testis-specific transcripts (fig. 5). Also other ubiquitously expressed genes were reported to produce testis-biased mRNA isoforms, e.g., hypoxia-inducible factor 1, alpha subunit *(Hif1a)*, platelet-activating factor acetylhydrolase, isoform 1b, beta1 subunit *(Pafah1b1)*, SH3-domain GRB2-like B1 *(Sh3glb1)*, and thioredoxin reductase 1 *(TXNRD1)* [Marti et al., 2002; Nayernia et al., 2003; Hrabchak et al., 2007; Dammeyer et al., 2008]. The presence of a testis-specific transcript could indicate that the *Npal3* gene is involved in male fertility. However, the analysis of *Npal3*$^{-/-}$ knockout animals did not demonstrate any fertility-relevant phenotype. Both *Npal3*$^{-/-}$ males and females were fertile; thus, the *Npal3* gene alone is not critical for male fertility despite its testis-specific transcript.

It was demonstrated that changes in mRNA levels of *NIPA1* and *NIPA2* in Prader-Willi patients correlated with intellectual ability [Bittel et al., 2006]. The *Npal3* gene encodes not only a protein with a similar structure in comparison to the NIPA proteins but also shows a strong expression in the brain. Similar findings were reported by Chai and coworkers [2003] for *Nipa1* in the mouse brain. Therefore, one could expect that the disruption of the *Npal3* gene could affect the behavior of *Npal3*$^{-/-}$ mice. Indeed, analysis of mutant *Npal3* females demonstrated changes in social affinity, and mutant *Npal3* males displayed deficits in exploratory behavior. It is a well known fact that genetic studies in the mouse are important for the elucidation of molecular pathways underlying behavior and psychiatric disorders [Tarantino and Bucan, 2000; Bucan and Abel 2002; Seong et al., 2002; Inoue and Lupski, 2003]. Recently, a brain-expressed NRG1 type IV protein, which possesses a transmembrane domain [Tan et al., 2007], has been linked to schizophrenia [Law et al., 2006]. Mutant mice lacking the *Nlgn4l* gene, which also encodes a transmembrane protein, exhibited deficits in reciprocal social interactions [Jamain et al., 2008]. In humans monosomy of the chromosomal region 1p36 is commonly observed in patients with mental retardation [for review see Battaglia, 2005; Gajecka et al., 2007]. Moreover, a patient presenting with a deletion of 1p36 exhibited a Prader-Willi-like syndrome [D'Angelo et al., 2006]. This latter observation could be an additional hint that the NPAL3 proteins might play a similar role as the NIPA proteins.

Mouse models have been a primary source of information for understanding the intricate mechanisms of the immune system [Bluethmann and Ohashi, 1994; Mak et al., 2001; Fischer, 2002; Rogner and Avner, 2003]. The immune system screen of *Npal3* mutant mice revealed a de-

crease of NK cells and significant differences in IgM, IgG_2, and IgA levels in *Npal3*$^{-/-}$ mice as compared to wildtype mice. However, these changes were minor and without any obvious tendencies. Therefore, further analyses are needed before any specific statement about the role of *Npal3* for the immune system can be made.

The increased production of IgE in response to common environmental antigens is the hallmark of atopic diseases in man [Hamelmann et al., 1999]. Sequence conservations between genes in mouse and human make mouse models suitable for studying the function of human genes [for review see Guenet, 2005]. Thus, because of the increased level of IgE in *Npal3*$^{-/-}$ males, this knockout line could serve as an interesting model for studying atopic diseases. Lima et al. [2008] demonstrated a link between asthma and a polymorphism in the human natriuretic peptide precursor A *(NPPA)* gene. The *NPPA* gene is located on human chromosome 1p36.21, in close distance to the *NPAL3* gene. Also in mouse both *Nppa* and *Npal3* genes are located in the syntenic region on chromosome 4D3. Interestingly, Haagerup et al. [2002] reported linkage of 1p36 with asthma, and moreover, seasonal allergic rhinitis (SAR) was also linked to this chromosomal region [Yokouchi et al., 2002]. In addition, a recent genome-wide linkage scan conducted in 110 families with asthmatic siblings revealed linkage of 1p36 to the value of forced expiratory volume in one second in the testing of lung function [Bouzigon et al., 2007]. In the *Npal3* knockout mouse line only males were affected; however, it should be pointed out that the difference between sexes in IgE level changes is a common finding in mouse inbred lines [Alessandrini et al., 2001; Seymour et al., 2002; Corteling and Trifilieff, 2004]. In humans a study about the association between allergic sensitization and several lifestyle/environmental factors demonstrated differences in IgE level between both genders [Linneberg et al., 2001]. It was also suggested that sex hormones could modify an immune response [Roitt and Rabson, 2000]. In addition, the exposure for the toxic effect of mercury chloride resulted in different IgE level changes in males and females [Hultman and Nielsen, 2001; Nielsen and Hultman, 2002]. The lung function was similarly affected only in mutant *Npal3* males. In general, the pathology of the respiratory system is a typical feature of asthma or chronic airway obstruction. For example, the transmembrane protein THIM (previously known as TIM-1) was reported to play a protective role against atopy in the mouse [McIntire et al., 2004]. Furthermore, the mRNA level of the *Adam8* gene, coding for another transmembrane protein, was shown to increase in lungs of mice after exposure to allergens [King et al., 2004]. Moreover, gender-related differences in asthma development and lung function were also reported [reviewed in Carey et al., 2007; Postma, 2007].

In summary, mouse and human *Npal3*/*NPAL3* genes are widely expressed, and the targeted disruption of the *Npal3* gene affects different physiological processes in mutant mice. However, additional and more detailed studies are needed to elucidate the exact function of the NPAL3 proteins.

Acknowledgments

We thank M. Schindler and H. Riedesel for their assistance in generation of the *Npal3* knockout mice and W. Engel for critical discussion and financial support. We thank the members of the German Mouse Clinic for comprehensive phenotyping of the *Npal3* knockout mice and fruitful discussions. We also like to thank S. Herold, R. Seeliger, C. Führmann-Franz, K. Kutzner, C. Schneider, and C. Zeller for their excellent technical assistance. This work was supported by a grant from the BMBF/German Ministry of Education and Science (NGFNplus: 01GS0850 to SMH, WW, IB, HS, HF, VG-D, and MHA; 01GS0852 to SK, TA and DB; 01GS0868 to AJ, AA and MO) and by an EU grant (LSHG-2006-037188, German Mouse Clinic). Data will be published on www.europhenome.org.

References

Alessandrini F, Jakob T, Wolf A, Wolf E, Balling R, et al: ENU Mouse Mutagenesis: generation of mouse mutants with aberrant plasma IgE levels. Int Arch Allergy Immunol 124: 25–28 (2001).

Altschul SF, Gish W, Miller W, Myers EW, Lipman DJ: Basic local alignment search tool. J Mol Biol 215:403–410 (1990).

Andersson B, Wentland MA, Ricafrente JY, Liu W, Gibbs RA: A 'double adaptor' method for improved shotgun library construction. Anal Biochem 236:107–113 (1996).

Battaglia A: Del 1p36 syndrome: a newly emerging clinical entity. Brain Dev 27:358–361 (2005).

Bittel DC, Kibiryeva N, Butler MG: Expression of 4 genes between chromosome 15 breakpoints 1 and 2 and behavioral outcomes in Prader-Willi syndrome. Pediatrics 118: e1276–e1283 (2006).

Bluethmann H, Ohashi PS: Transgenesis and Targeted Mutagenesis in Immunology (Academic Press, San Diego 1994).

Bonaldo MF, Lennon G, Soares MB: Normalization and subtraction: two approaches to facilitate gene discovery. Genome Res 6:791–806 (1996).

Bouzigon E, Siroux V, Dizier MH, Lemainque A, Pison C, et al: Scores of asthma and asthma severity reveal new regions of linkage in EGEA study families. Eur Respir J 30:253–259 (2007).

Bucan M, Abel T: The mouse: genetics meets behaviour. Nat Rev Genet 3:114–123 (2002).

Butler MG: Prader-Willi syndrome: current understanding of cause and diagnosis. Am J Med Genet 35:319–332 (1990).

Butler MG, Bittel DC, Kibiryeva N, Talebizadeh Z, Thompson T: Behavioral differences among subjects with Prader-Willi syndrome and type I or type II deletion and maternal disomy. Pediatrics 113:565–573 (2004).

Carey MA, Card JW, Voltz JW, Arbes SJ Jr, Germolec DR, et al: It's all about sex: gender, lung development and lung disease. Trends Endocrinol Metab 18:308–313 (2007).

Chai JH, Locke DP, Greally JM, Knoll JH, Ohta T, et al: Identification of four highly conserved genes between breakpoint hotspots BP1 and BP2 of the Prader-Willi/Angelman syndromes deletion region that have undergone evolutionary transposition mediated by flanking duplicons. Am J Hum Genet 73: 898–925 (2003).

Corteling R, Trifilieff A: Gender comparison in a murine model of allergen-driven airway inflammation and the response to budesonide treatment. BMC Pharmacol 4:4 (2004).

Dammeyer P, Damdimopoulos AE, Nordman T, Jiménez A, Miranda-Vizuete A, Arnér ES: Induction of cell membrane protrusions by the N-terminal glutaredoxin domain of a rare splice variant of human thioredoxin reductase 1. J Biol Chem 283:2814–2821 (2008).

D'Angelo CS, Da Paz JA, Kim CA, Bertola DR, Castro CI, et al: Prader-Willi-like phenotype: investigation of 1p36 deletion in 41 patients with delayed psychomotor development, hypotonia, obesity and/or hyperphagia, learning disabilities and behavioral problems. Eur J Med Genet 49:451–460 (2006).

Drorbaugh JE, Fenn WO: A barometric method for measuring ventilation in newborn infants. Pediatrics 16:81–87 (1955).

Fischer A: Natural mutants of the immune system: a lot to learn! Eur J Immunol 32:1519–1523 (2002).

Gailus-Durner V, Fuchs H, Becker L, Bolle I, Brielmeier M, et al: Introducing the German Mouse Clinic: open access platform for standardized phenotyping. Nat Methods 2:403–404 (2005).

Gajecka M, Mackay KL, Shaffer LG: Monosomy 1p36 deletion syndrome. Am J Med Genet C Semin Med Genet 145C:346–356 (2007).

Goytain A, Quamme GA: Identification and characterization of a novel mammalian Mg^{2+} transporter with channel-like properties. BMC Genomics 6:48 (2005).

Goytain A, Hines RM, El-Husseini A, Quamme GA: *NIPA1(SPG6)*, the basis for autosomal dominant form of hereditary spastic paraplegia, encodes a functional Mg^{2+} transporter. J Biol Chem 282:8060–8068 (2007).

Goytain A, Hines RM, Quamme GA: Functional characterization of NIPA2, a selective Mg^{2+} transporter. Am J Physiol Cell Physiol 295:C944–C953 (2008).

Gregory SG, Barlow KF, McLay KE, Kaul R, Swarbreck D, et al: The DNA sequence and biological annotation of human chromosome 1. Nature 441:315–321 (2006).

Guenet JL: The mouse genome. Genome Res 15: 1729–1740 (2005).

Haagerup A, Bjerke T, Schiøtz PO, Binderup HG, Dahl R, Kruse TA: Asthma and atopy – a total genome scan for susceptibility genes. Allergy 57:680–686 (2002).

Hamelmann E, Tadeda K, Oshiba A, Gelfand EW: Role of IgE in the development of allergic airway inflammation and airway hyperresponsiveness – a murine model. Allergy 54:297–305 (1999).

Hodge R: Preparation of RNA gel blots. Methods Mol Biol 28:49–54 (1994).

Hrabchak C, Henderson H, Varmuza S: A testis specific isoform of endophilin B1, endophilin B1t, interacts specifically with protein phosphatase-1cγ2 in mouse testis and is abnormally expressed in PP1cγ null mice. Biochemistry 46:4635–4644 (2007).

Hultman P, Nielsen JB: The effect of dose, gender, and non-H-2 genes in murine mercury-induced autoimmunity. J Autoimmun 17: 27–30 (2001).

Inoue K, Lupski JR: Genetics and genomics of behavioral and psychiatric disorders. Curr Opin Genet Dev 13:303–309 (2003).

Jamain S, Radyushkin K, Hammerschmidt K, Granon S, Boretius S, et al: Reduced social interaction and ultrasonic communication in a mouse model of monogenic heritable autism. Proc Natl Acad Sci USA 105:1710–1715 (2008).

Joyner A: Production of embryonic stem cell clones; in Wurst W, Joyner A (eds): Gene Targeting: A Practical Approach, pp 33–61 (IRL Press, New York 1993).

King NE, Zimmermann N, Pope SM, Fulkerson PC, Nikolaidis NM, et al: Expression and regulation of a disintegrin and metalloproteinase (ADAM) 8 in experimental asthma. Am J Respir Cell Mol Biol 31:257–265 (2004).

Kopczynski CC, Noordermeer JN, Serano TL, Chen WY, Pendleton JD, et al: A high throughput screen to identify secreted and transmembrane proteins involved in *Drosophila* embryogenesis. Proc Natl Acad Sci USA 95:9973–9978 (1998).

Kozak M: Initiation of translation in prokaryotes and eukaryotes. Gene 234:187–208 (1999).

Law AJ, Lipska BK, Weickert CS, Hyde TM, Straub RE, et al: Neuregulin 1 transcripts are differentially expressed in schizophrenia and regulated by 5′ SNPs associated with the disease. Proc Natl Acad Sci USA 103:6747–6752 (2006).

Lichter P, Cremer T, Borden J, Manuelidis L, Ward DC: Delineation of individual human chromosomes in metaphase and interphase cells by in situ suppression hybridization using recombinant DNA libraries. Hum Genet 80:224–234 (1988).

Lima JJ, Mohapatra S, Feng H, Lockey R, Jena PK, et al: A polymorphism in the *NPPA* gene associates with asthma. Clin Exp Allergy 38: 1117–1123 (2008).

Linneberg A, Nielsen NH, Madsen F, Frølund L, Dirksen A, Jørgensen T: Factors related to allergic sensitization to aeroallergens in a cross-sectional study in adults: The Copenhagen Allergy Study. Clin Exp Allergy 9: 1409–1417 (2001).

Mak TW, Penninger JM, Ohashi PS: Knockout mice: a paradigm shift in modern immunology. Nat Rev Immunol 1:11–19 (2001).

Marti HH, Katschinski DM, Wagner KF, Schäffer L, Stier B, Wenger RH: Isoform-specific expression of hypoxia-inducible factor-1α during the late stages of mouse spermiogenesis. Mol Endocrinol 16:234–243 (2002).

McIntire JJ, Umetsu DT, DeKruyff RH: *TIM-1*, a novel allergy and asthma susceptibility gene. Springer Semin Immunopathol 25:335–348 (2004).

Meijer D, Hermans A, von Lindern M, van Agthoven T, de Klein A, et al: Molecular characterization of the testis specific *c-abl* mRNA in mouse. EMBO J 6:4041–4048 (1987).

Moller S, Croning MD, Apweiler R: Evaluation of methods for the prediction of membrane spanning regions. Bioinformatics 17:646–653 (2001).

Nayernia K, Vauti F, Meinhardt A, Cadenas C, Schweyer S, et al: Inactivation of a testis-specific Lis1 transcript in mice prevents spermatid differentiation and causes male infertility. J Biol Chem 278:48377–48385 (2003).

Nicholls RD, Knepper JL: Genome organization, function, and imprinting in Prader-Willi and Angelman syndromes. Annu Rev Genomics Hum Genet 2:153–175 (2001).

Nicholls RD, Gottlieb W, Russell LB, Davda M, Horsthemke B, Rinchik EM: Evaluation of potential models for imprinted and nonimprinted components of human chromosome 15q11-q13 syndromes by fine-structure homology mapping in the mouse. Proc Natl Acad Sci USA 90:2050–2054 (1993).

Nielsen JB, Hultman P: Mercury-induced autoimmunity in mice. Environ Health Perspect 110 (suppl 5):877–881 (2002).

Ohl F, Sillaber I, Binder E, Keck ME, Holsboer F: Differential analysis of behavior and diazepam-induced alterations in C57BL/6N and BALB/c mice using the modified hole board test. J Psychiatr Res 35:147–154 (2001).

Oyen O, Myklebust F, Scott JD, Cadd GG, McKnight GS, et al: Subunits of cyclic adenosine 3′,5′-monophosphate-dependent protein kinase show differential and distinct expression patterns during germ cell differentiation: alternative polyadenylation in germ cells gives rise to unique smaller-sized mRNA species. Biol Reprod 43:46–54 (1990).

Postma DS: Gender differences in asthma development and progression. Gend Med 4 Suppl B:133–146 (2007).

Rainier S, Chai JH, Tokarz D, Nicholls RD, Fink JK: *NIPA1* gene mutations cause autosomal dominant hereditary spastic paraplegia (SPG6). Am J Hum Genet 73:967–971 (2003).

Rapp G, Klaudiny J, Hagendorff G, Luck MR, Scheit KH: Complete sequence of the coding region of human elongation factor 2 *(EF-2)* by enzymatic amplification of cDNA from human ovarian granulosa cells. Biol Chem Hoppe Seyler 370:1071–1075 (1989).

Rogner UC, Avner P: Congenic mice: cutting tools for complex immune disorders. Nat Rev Immunol 3:243–252 (2003).

Roitt I, Rabson A: Autoimmune diseases, in Roitt I, Rabson A (eds): Really Essential Medical Immunology, pp 160–168 (Blackwell Science, Oxford 2000).

Rosahl TW, Spillane D, Missler M, Herz J, Selig DK, et al: Essential functions of synapsins I and II in synaptic vesicle regulation. Nature 375:488–493 (1995).

Seong E, Seasholtz AF, Burmeister M: Mouse models for psychiatric disorders. Trends Genet 18:643–650 (2002).

Seymour BW, Friebertshauser KE, Peake JL, Pinkerton KE, Coffman RL, Gershwin LJ: Gender differences in the allergic response of mice neonatally exposed to environmental tobacco smoke. Dev Immunol 9:47–54 (2002).

Tan W, Wang Y, Gold B, Chen J, Dean M, et al: Molecular cloning of a brain-specific, developmentally regulated neuregulin 1 *(NRG1)* isoform and identification of a functional promoter variant associated with schizophrenia. J Biol Chem 282:24343–24351 (2007).

Tarantino LM, Bucan M: Dissection of behavior and psychiatric disorders using the mouse as a model. Hum Mol Genet 9:953–965 (2000).

Wallace AM, Dass B, Ravnik SE, Tonk V, Jenkins NA, et al: Two distinct forms of the 64,000 Mr protein of the cleavage stimulation factor are expressed in mouse male germ cells. Proc Natl Acad Sci USA 96:6763–6768 (1999).

Wang X, Shaw WR, Tsang HT, Reid E, O'Kane CJ: *Drosophila* spichthyin inhibits BMP signaling and regulates synaptic growth and axonal microtubules. Nat Neurosci 10:177–185 (2007).

Wurst W, Goyner A: Production of targeted embryonic stem cell clones; in Goyner AL (ed): Gene Targeting: A Practical Approach, pp 33–61 (IRL Press, Oxford 1993).

Yokouchi Y, Shibasaki M, Noguchi E, Nakayama J, Ohtsuki T, et al: A genome-wide linkage analysis of orchard grass-sensitive childhood seasonal allergic rhinitis in Japanese families. Genes Immun 3:9–13 (2002).

Zornig M, Klett C, Lovec H, Hameister H, Winking H, et al: Establishment of permanent wild-mouse cell lines with readily identifiable marker chromosomes. Cytogenet Cell Genet 71:37–40 (1995).

Erratum

In the article of Grzmil et al. 'Targeted Disruption of the Mouse *Npal3* Gene Leads to Deficits in Behavior, Increased IgE Levels, and Impaired Lung Function' (Cytogenet Genome Res 2009;125:186–200) some of the authors' names and affiliations are incorrect.

These are the correct names and affiliations:

P. Grzmil[a, b] J. Konietzko[a] D. Boehm[a] S.M. Hölter[c] A. Aguilar-Pimentel[d, e] A. Javaheri[d, e] S. Kalaydjiev[d, f, g] T. Adler[d, f] I. Bolle[h] I. Adham[a] C. Dixkens[a] S. Wolf[a] H. Fuchs[d] V. Gailus-Durner[d] W. Wurst[c, i] M. Ollert[e] D.H. Busch[f] H. Schulz[h] M. Hrabé de Angelis[d, j] P. Burfeind[a]

[a] Institute of Human Genetics, University of Goettingen, Goettingen, Germany;
[b] Department of Genetics and Evolution, Institute of Zoology, Jagiellonian University, Cracow, Poland;
[c] Institute of Developmental Genetics, Helmholtz Zentrum München, Neuherberg, Germany;
[d] German Mouse Clinic, Institute of Experimental Genetics, Helmholtz Zentrum München, Neuherberg, Germany;
[e] Division of Environmental Dermatology and Allergy (UDA), Helmholtz Zentrum München/Technische Universität München, and Clinical Research Division of Molecular and Clinical Allergotoxicology, Department of Dermatology and Allergy, Technische Universität München, München, Germany;
[f] Institute for Medical Microbiology, Immunology and Hygiene, Technische Universität München, München, Germany;
[g] Miltenyi Biotec Ltd., Bisley, UK;
[h] Institute of Lung Biology and Disease, Helmholtz Zentrum München, Neuherberg, Germany;
[i] Chair of Developmental Genetics, Center of Life and Food Sciences Weihenstephan, Technische Universität München, Freising, Germany;
[j] Chair of Experimental Genetics, Center of Life and Food Sciences Weihenstephan, Technische Universität München, Freising, Germany